

University of Wollongong

Research Online

---

Faculty of Engineering and Information  
Sciences - Papers: Part B

Faculty of Engineering and Information  
Sciences

---

2019

## Persulfate oxidation-assisted membrane distillation process for micropollutant degradation and membrane fouling control

Muhammad Bilal Asif  
*University of Wollongong, mba409@uowmail.edu.au*

Zulqarnain Fida  
*University of Wollongong, zf866@uowmail.edu.au*

Arbab Tufail  
*University of Wollongong, at742@uowmail.edu.au*

Jason Van Der Merwe  
*Griffith University*

Frederic Leusch  
*Griffith University*

*See next page for additional authors*

Follow this and additional works at: <https://ro.uow.edu.au/eispapers1>

 Part of the [Engineering Commons](#), and the [Science and Technology Studies Commons](#)

---

### Recommended Citation

Asif, Muhammad Bilal; Fida, Zulqarnain; Tufail, Arbab; Van Der Merwe, Jason; Leusch, Frederic; Pramanik, Biplob K.; Price, William E.; and Hai, Faisal I., "Persulfate oxidation-assisted membrane distillation process for micropollutant degradation and membrane fouling control" (2019). *Faculty of Engineering and Information Sciences - Papers: Part B*. 2620.  
<https://ro.uow.edu.au/eispapers1/2620>

Research Online is the open access institutional repository for the University of Wollongong. For further information contact the UOW Library: [research-pubs@uow.edu.au](mailto:research-pubs@uow.edu.au)

---

# Persulfate oxidation-assisted membrane distillation process for micropollutant degradation and membrane fouling control

## Abstract

In this study, long-term performance of a persulfate (PS)-assisted direct contact membrane distillation (DCMD) process was examined for the treatment of secondary treated effluent spiked with a mixture of micropollutants including three pesticides and nine pharmaceuticals. A stand-alone DCMD ('control') was also operated under identical operating conditions for comparison. Depending on the micropollutant, the stand-alone DCMD achieved 86 to >99% removal. In comparison, removal by the PS-assisted DCMD was >99% for all investigated micropollutants. This was attributed to the fact that sulfate radicals (SO<sub>4</sub><sup>-</sup>) formed following the activation of PS at the DCMD operating temperature (i.e., 40 °C) achieved micropollutant-specific degradation, which reduced the accumulation of micropollutants in the feed. Chemical structures of the micropollutants governed their degradation by PS. Effective degradation (>90%) was achieved for micropollutants that contain strong electron-donating functional groups (EDGs) in their molecules (e.g., amitriptyline and trimethoprim). Micropollutants containing both strong electron-withdrawing functional groups (EWGs) and EDGs in their molecules were moderately degraded (60-80%). In addition to the micropollutants, activated PS significantly degraded total organic carbon (70%) and total nitrogen (40%) from the secondary treated wastewater. This helped to reduce the fouling layer on the membrane-surface in the PS-assisted DCMD system. PS-addition appears to slightly increase the toxicity of wastewater, but with effective retention of PS and degradation products, DCMD permeate (i.e., treated effluent) was not toxic. This is the first study demonstrating the performance of the persulfate oxidation process in a continuous-flow membrane system for micropollutant removal and membrane fouling control.

## Keywords

oxidation-assisted, membrane, distillation, persulfate, process, control, micropollutant, degradation, fouling

## Disciplines

Engineering | Science and Technology Studies

## Publication Details

Asif, M. B., Fida, Z., Tufail, A., Van Der Merwe, J., Leusch, F. D. L., Pramanik, B. K., Price, W. E. & Hai, F. I. (2019). Persulfate oxidation-assisted membrane distillation process for micropollutant degradation and membrane fouling control. *Separation and Purification Technology*, 222 321-331.

## Authors

Muhammad Bilal Asif, Zulqarnain Fida, Arbab Tufail, Jason Van Der Merwe, Frederic Leusch, Biplob K. Pramanik, William E. Price, and Faisal I. Hai

**Persulfate oxidation-assisted membrane distillation process for micropollutant degradation and membrane fouling control**

(Accepted manuscript)

**Muhammad B. Asif<sup>a</sup>, Zulqarnain Fida<sup>a</sup>, Arbab Tufail<sup>a</sup>, Jason P. van de Merwe<sup>b</sup>, Frederic D.L. Leusch<sup>b</sup>, Biplob K. Pramanik<sup>a,c</sup>, William E. Price<sup>d</sup>, Faisal I. Hai<sup>a,\*</sup>**

<sup>a</sup> Strategic Water Infrastructure Laboratory, School of Civil, Mining and Environmental Engineering, University of Wollongong, Wollongong, NSW 2522, Australia.

<sup>b</sup> Australian Rivers Institute and School of Environment and Science, Griffith University, QLD 4222, Australia.

<sup>c</sup> Civil and Infrastructure Engineering, School of Engineering, RMIT University, Australia

<sup>d</sup> Strategic Water Infrastructure Lab, School of Chemistry, University of Wollongong, Wollongong, NSW 2522, Australia.

\* **Corresponding Author:** [faisal@uow.edu.au](mailto:faisal@uow.edu.au); Tel.: +61-2-42213054

**Publication details:**

Asif, M.B., Fida, Z., Tufail, A., van de Merwe, J.P., Leusch, F.D.L., Pramanik, B.K., Price, W.E., Hai, F.I. 2019. Persulfate oxidation-assisted membrane distillation process for micropollutant degradation and membrane fouling control. *Separation and Purification Technology*, **222**, 321-331.

**Highlights:**

- Combined persulfate (PS)-membrane distillation improves micropollutant (MP) removal
- MP properties governed their degradation by PS from secondary treated wastewater
- MP degradation by PS led to their consistent removal by membrane
- Effluent organic matter degradation by PS helped mitigate membrane fouling
- Final treated water was non-toxic as confirmed by bioluminescence toxicity assay

**Abstract:**

In this study, long-term performance of a persulfate (PS)-assisted direct contact membrane distillation (DCMD) process was examined for the treatment of secondary treated effluent spiked with a mixture of micropollutants including three pesticides and nine pharmaceuticals. A stand-alone DCMD ('control') was also operated under identical operating conditions for comparison. Depending on the micropollutant, the stand-alone DCMD achieved 86 to >99% removal. In comparison, removal by the PS-assisted DCMD was >99% for all investigated micropollutants. This was attributed to the fact that sulfate radicals ( $\text{SO}_4^{\cdot -}$ ) formed following the activation of PS at the DCMD operating temperature (*i.e.*, 40 °C) achieved micropollutant-specific degradation, which reduced the accumulation of micropollutants in the feed. Chemical structures of the micropollutants governed their degradation by PS. Effective degradation (>90%) was achieved for micropollutants that contain strong electron-donating functional groups (EDGs) in their molecules (*e.g.*, amitriptyline and trimethoprim). Micropollutants containing both strong electron-withdrawing functional groups (EWGs) and EDGs in their molecules were moderately degraded (60-80%). In addition to the micropollutants, activated PS significantly degraded total organic carbon (70%) and total nitrogen (40%) from the secondary treated wastewater. This helped to reduce the fouling layer on the membrane-surface in the PS-assisted DCMD system. PS-addition appears to slightly increase the toxicity of wastewater, but with effective retention of PS and degradation products, DCMD permeate (*i.e.*, treated effluent) was not toxic. This is the first study demonstrating the performance of the persulfate oxidation process in a continuous-flow membrane system for micropollutant removal and membrane fouling control.

**Keywords:** heat-activated persulfate; mass transfer coefficient, membrane distillation; membrane fouling; micropollutants; sulphate radicals, toxicity analysis

## 1. Introduction

Micropollutants such as pharmaceuticals and pesticides are organic contaminants that are ubiquitous in wastewater at trace concentrations, *i.e.*, from nanogram to up to a few micrograms per litre [1, 2]. Current biological wastewater treatment processes such as the conventional activated sludge process and membrane bioreactors (MBR) are effective only for a few specific groups of micropollutants [3], particularly hydrophobic and/or readily degradable micropollutants, *i.e.*, those containing electron-donating functional groups (EDGs). On the other hand, micropollutants that are either structurally complex or contain an electron-withdrawing functional group (EWG) in their molecule are resistant to biodegradation. Among different classes of micropollutants, pharmaceuticals (*e.g.*, carbamazepine and diclofenac) and pesticides (*e.g.*, atrazine and linuron) that generally contain strong EWGs in their molecules are poorly degraded by activated sludge, consequently resulting in their occurrence in secondary treated effluent [4-6]. This raises significant concern due to their potential harmful impact on aquatic organisms and even humans in the case of prolonged ingestion. Therefore, an effective tertiary treatment process is required for removal of micropollutants such as pharmaceuticals and pesticides, to produce product water suitable for safe disposal and reuse.

Recently membrane distillation (MD) has gained significant attention as an effective separation process [7, 8]. MD is a thermally driven membrane separation process; however, it requires a lower operating temperature than conventional distillation processes such as fractional distillation. During the MD process, water in vapour form moves *via* diffusion through a microporous hydrophobic membrane from a higher temperature feed solution to a lower temperature permeate solution. This occurs due to the vapour pressure gradient developed by the temperature difference between the sides of the membrane [9, 10]. Since the water moves across the membrane in vapour form, MD can theoretically provide complete removal of non-volatile pollutants [7, 11, 12]. Furthermore, the compatibility of the MD process with low-grade waste heat and solar thermal energy [9] makes its application attractive in various fields, including water desalination and wastewater treatment.

The MD process has been predominantly assessed for the desalination of sea and brackish water, particularly for hyper-saline feed, because, being a thermally driven process, water flux in MD is negligibly affected by the feed osmotic pressure as compared to the pressure-driven membrane desalination processes (*e.g.*, RO and NF) [8, 13, 14]. Despite the potential to date, the performance of MD for the removal of micropollutants has been assessed only in a few short-term batch studies. For instance, Wijekoon et al. [7] investigated the removal of micropollutants including pesticides and pharmaceuticals by MD operated in batch mode for 24h. They observed micropollutant removal to be governed by their volatility and hydrophobicity. In another short-term study by Han et al. [15], MD achieved 90-95% removal of a nonsteroidal anti-inflammatory drug ibuprofen from synthetic wastewaters mimicking surface water or reverse-osmosis concentrate. Although these studies provide useful insights, it is important to note that a continuous-flow operation is required to analyse and

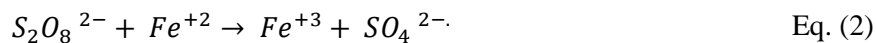
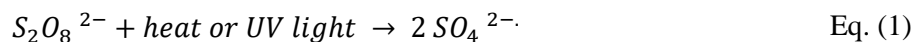
understand process stability. To date, only a handful of studies have assessed micropollutant removal in continuous-flow mode [8, 16]. The authors reported 70 to 99% removal of the investigated micropollutants depending on their physicochemical properties. Two particular aspects highlighted in these studies were: (a) membrane fouling, significantly reducing permeate flux; and (b) additional requirement of treatment and disposal of membrane-concentrate rich in micropollutants as well as other organic and inorganic impurities.

Unlike pressure-driven membrane separation processes such as ultrafiltration and nanofiltration, strategies for the mitigation of MD membrane fouling during treatment of secondary treated effluent have not been studied to date. To control fouling of pressure-driven membranes, augmentation of different physicochemical processes such as activated carbon adsorption [17], coagulation [18] and advanced oxidation processes [19, 20] have been assessed. While these physicochemical processes can help reduce membrane fouling by removing the residual organic matter from secondary treated effluent [21, 22], the suitability of these techniques is case-specific. For example, coagulation may not effectively remove hydrophilic and low molecular weight organic matter that could cause membrane fouling *via* pore blockage mechanism [22, 23]. Adsorption can remove low molecular weight organic matters more effectively [17, 21, 24]; however, some studies report an adverse impact of activated carbon dosing to membrane reactors. For instance, Shao et al. [25] investigated a combined powdered activated carbon (PAC) – ultrafiltration process for membrane fouling mitigation during the treatment of surface water. They observed that the interaction of PAC with humic substances led to the formation of a combined fouling layer on the surface of the ultrafiltration membrane, which caused rapid membrane fouling [25]. Notably, both coagulation and adsorption remove organic matters by transferring them from water to a solid phase. Therefore, disposal of the large quantities of toxic sludge or solid waste produced is a serious concern.

Among the advanced oxidation processes, ozonation has been mostly investigated for pressure-driven membrane fouling control [26, 27]. Ozonation can also degrade micropollutants commonly detected in secondary treated effluent [1, 28]. However, ozone residuals may interact with membrane material, and can reduce the membrane lifetime [29]. Activated persulfate (PS) is an emerging advanced oxidation process that can degrade both natural organic matter and recalcitrant micropollutants including pharmaceuticals and pesticides [30, 31]. Therefore, it is reasonable to envisage that activated PS can simultaneously degrade micropollutants and organic foulants during MD operation. However, this has not been verified yet.

PS is stable at room temperature, but can be activated by various agents such as transition metals (*e.g.*, iron), heat, and ultraviolet (UV) light to form one or more sulphate radicals ( $\text{SO}_4^{\cdot -}$ ), which are highly reactive [30]. PS activation by heat and UV light produce two  $\text{SO}_4^{\cdot -}$  radicals (Equation 1), while only one  $\text{SO}_4^{\cdot -}$  radical is generated following activation by transition metals such as  $\text{Fe}^{2+}$  (Equation 2). This

indicates that activation by heat or UV light may provide more efficient treatment compared to activation by a transition metal [30, 32].



PS activated by UV light was reported to control fouling during the treatment of surface water by an ultrafiltration membrane [21]. In another study by Chen et al. [33], fouling of an ultrafiltration membrane caused by humic substances and sodium alginate was significantly reduced by peroxymonosulfate activated by  $Fe^{2+}$ . In addition, the combined peroxymonosulfate (50  $\mu\text{M}$ ) –  $Fe^{2+}$  (50  $\mu\text{M}$ ) process achieved above 99% degradation of atrazine, outperforming atrazine removal by coagulation [33]. Heat activated PS has been also reported to achieve 40-100% removal of a few investigated micropollutants such as atrazine, aniline, monochlorobenzene and 2,4-dichlorophenol [30].

Since the temperature of the feed solution is usually kept at 40-45°C during the treatment of secondary treated effluent by MD [7, 16], an additional PS activator will not be required for generation of sulphate radicals. This makes PS a suitable candidate to be integrated with MD. A thorough literature survey suggests that an integrated PS-assisted MD process has not been investigated for micropollutant removal and membrane fouling control. To-date, research related to persulfate oxidation process has mainly focused on PS activation and the identification of radicals. In terms of micropollutant removal, most PS studies assessed degradation of single micropollutants at concentrations significantly higher than that environmentally relevant [34, 35]. Since wastewater contains a wide range of micropollutants at trace concentration, it seems more suitable to assess PS performance for the degradation of micropollutant mixtures at environmentally relevant concentrations.

This study was conducted with an aim to assess the performance and stability of a PS-assisted MD process for the treatment of secondary treated effluent (*i.e.*, MBR permeate). The fate of nine pharmaceuticals and personal care products (PPCPs) and three pesticides during the PS-assisted MD was investigated and compared to a ‘control’ MD process (without PS). Basic water quality parameters such as total organic carbon (TOC) and total nitrogen (TN) as well as membrane water productivity was thoroughly evaluated to determine the fouling behaviour. At the end of operation with and without PS dosing, MD membranes were characterized by scanning electron microscopy (SEM) - energy dispersion spectrometry (EDS) to gain an in-depth understanding of the fouling control achieved by PS.

## 2. Material and methods

### 2.1. Chemicals

Potassium persulfate (PS) was purchased from Sigma-Aldrich (Australia). The stock solution (100 mM) of PS was prepared in ultrapure Milli-Q water and stored at 4°C before use. HPLC grade acetonitrile, methanol, dichloromethane and formic acid were used for quantification of micropollutants as



explained in Section 2.4.2. As noted in Section 2.3.2, analytical grade glucose, peptone, urea, monopotassium phosphate, magnesium sulphate, ferrous sulphate, and sodium acetate were used to make the synthetic wastewater for MBR. The permeate of the MBR was used as feed for the MD system.

The feed to the MD system was dosed with 12 micropollutants including three pesticides and nine PPCPs (Table 1). These were selected based on their widespread occurrence in municipal wastewater and their reported ineffective removal by biological wastewater treatment plants including MBRs [1, 4]. These chemicals were also purchased from Sigma-Aldrich (Australia). A combined stock solution of micropollutants was prepared in pure methanol and stored at  $-18^{\circ}\text{C}$  in dark. Relevant physicochemical properties of the selected micropollutants are presented in Table 1, while their chemical structures are given in Supplementary Data Table S1.

**Table 1.** Physicochemical properties of micropollutants selected for this study

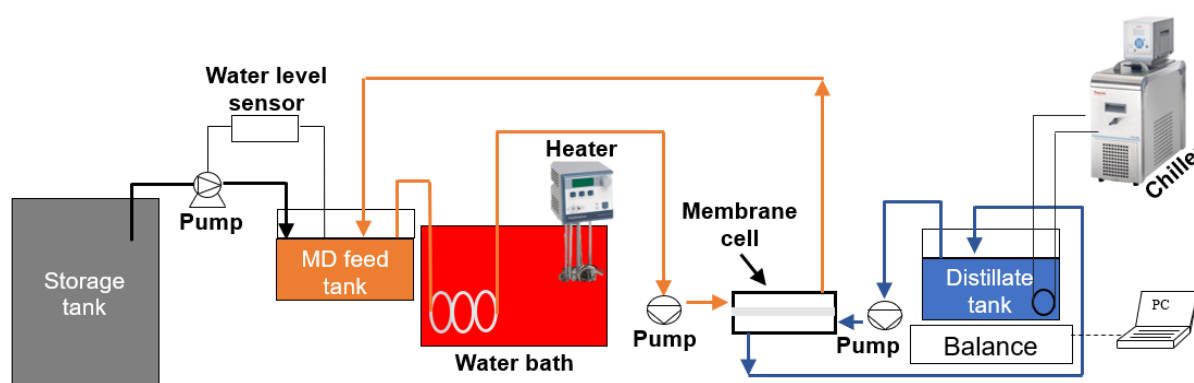
Type	Name	Molecular weight <sup>a</sup> (g/mol)	log D @ pH=7 <sup>a</sup>	pK <sub>a</sub> <sup>a</sup>	pK <sub>H</sub> @ pH=7 <sup>b</sup>	Charge at pH=7	
Pharmaceuticals and personal care products (PPCPs)	Acetaminophen	152	0.46	0.52	8.3	Negative	
	Bezafibrate	362	-0.93	3.29	-		
	Diclofenac	296	1.77	4.18	11.51		
	Sulfamethoxazole	253	-0.96	5.18	11.81		
	Amitriptyline	277	2.28	9.18	8.18		
	Carbamazepine	236	1.89	13.94	9.09		
	Primidone	218	0.83	12.26	13.93		
Pesticide	Triclosan	290	5.28	7.8	6.18	Neutral	
	Trimethoprim	290	0.27	7.04	13.62		
	Atrazine	216	2.64	2.27	7.28		Negative
	Linuron	249	3.12	12.13	8.71		
	Pentachlorophenol	266	2.85	4.68	7.59		

<sup>a</sup> molecular weight, log D (water partition coefficient) and pK<sub>a</sub> (acid dissociation coefficient) were obtained from the SciFinder Scholar database

<sup>b</sup> pK<sub>H</sub> = - log<sub>10</sub> H, where H is Henry's law constant and defined as vapour pressure×molecular weight/water solubility.  
“-”: not available

## 2.2. Experimental setup

A laboratory-scale direct contact membrane distillation (DCMD) system was used for the treatment of secondary treated effluent (Figure 1), due to the ease of operation as compared to other MD configurations, *e.g.*, air gap MD [9]. The DCMD setup consisted of a 3 L glass reactor (hereafter referred to as MD feed tank), a membrane module, a glass distillate tank (5 L) and two circulation gear pumps (Micropump Inc., Vancouver, WA, USA). Operated *via* a water level controller, a peristaltic pump (Cole-Parmer, Vernon Hills, IL, USA) supplied secondary treated water from a storage tank to the MD feed tank. The temperature of the MD feed tank, which was covered, was maintained at 40 ± 1.5°C by using a heating immersion circulator (Julabo, Seelbach, Germany), while a chiller (Thermo Scientific, Waltham, MA, USA) was used to keep the temperature of the distillate tank at 20 ± 0.5°C.

**Figure 1.** Schematic representation of the laboratory-scale DCMD setup used in this study

The MD membrane module was made of acrylic plastic. It was comprised of two identical cells, each engraved with flow channels 145 mm long, 95 mm wide and 3 mm deep as described previously [36].

A hydrophobic polytetrafluoroethylene (PTFE) membrane with a thickness, nominal pore size, and porosity of 60  $\mu\text{m}$ , 0.2  $\mu\text{m}$ , and 80%, respectively, was purchased from Ningbo Porous Membrane Technology (Ningbo, China). The media from the MD feed tank and the distillate tank were passed through the opposite membrane cells at a recirculation flowrate of 1 L/min (corresponding to a cross flow velocity of 9 cm/s) using two rotameters. The partial vapour pressure gradient developed due to difference in temperature allows water to move across the membrane as vapour, consequently increasing the volume of water in distillate tank. This tank was placed on a precision balance (Mettler-Toledo, Kings Park, NSW, Australia). Change in the weight of distillate water was recorded in a computer via BalanceLink software (Mettler Toledo) to determine the MD water flux.

## 2.3. Experimental protocol

### 2.3.1. DCMD process characterization

The DCMD process was characterised by calculating the mass transfer coefficient ( $K_m$ ) using a procedure previously described by Duong et al. [10]. Briefly, the DCMD system was operated in batch mode at different feed temperatures (*i.e.*, 40, 45 and 50  $^{\circ}\text{C}$ ) for 1 h with ultrapure Milli Q water. Distillate temperature was kept constant at 20  $^{\circ}\text{C}$ , and recirculation flow rate of both feed and distillate was maintained at 1 L/min. The permeate flux was recorded every 5 min for 1 h.

Permeate flux of DCMD can be theoretically calculated using Equation 3 as given below:

$$J = K_m \times (P_{feed} - P_{distillate}) \quad \text{Eq. (3)}$$

where  $J$  is the permeate flux ( $\text{L}/\text{m}^2 \text{ h}$ ) of DCMD,  $K_m$  is the mass transfer coefficient ( $\text{L}/\text{m}^2 \text{ h Pa}$ ),  $P_{feed}$  is the vapor pressure of water in MD feed, and  $P_{distillate}$  is the vapor pressure of water in MD distillate.  $P_{feed}$  and  $P_{distillate}$  can be determined by using Equation 4 [37]:

$$P = x_{water} \times \alpha_{water} \times P_o \quad \text{Eq. (4)}$$

where  $x_{water}$  and  $\alpha_{water}$  are the molar fraction and activity of water, respectively, and  $P_o$  is the vapor pressure of water in MD feed and distillate. Since DCMD was characterised with ultrapure Milli-Q water, value of both  $x_{water}$  and  $\alpha_{water}$  is equal to 1. Vapor pressure of water in MD feed and distillate can be calculated by using Antoine's Equation [10, 37] as given below:

$$P_o = \exp\left(23.1964 - \frac{3816.44}{T - 46.13}\right) \quad \text{Eq. (5)}$$

where  $T$  is the absolute temperature of the feed or distillate streams.

### 2.3.2. Treatment of secondary effluent by DCMD

Secondary treated effluent from a lab-scale MBR was collected for further treatment by DCMD. The MBR was operated for around one year while it was continuously fed with synthetic wastewater

containing 400 mg/L glucose, 100 mg/L peptone, 35 mg/L urea, 17.5 mg/L monopotassium phosphate, 17.5 mg/L magnesium sulphate, 10 mg/L ferrous sulphate, and 225 mg/L sodium acetate. The wastewater had a chemical oxygen demand (COD), total organic carbon (TOC), total nitrogen (TN) and  $\text{PO}_4^{3-}\text{-P}$  concentrations of 650, 175, 25, and 15 mg/L, respectively. The hydraulic retention time (HRT) and solids retention time of the MBR was 12 h and 10 d, respectively. Characteristics of the secondary effluent (*i.e.*, MBR permeate) to be treated by DCMD are given in Table 2.

**Table 2.** Characteristics of secondary treated effluent *i.e.*, DCMD feed (n = 10).

Parameter	Unit	Value (minimum – maximum)
pH	-	6.84 – 7.2
Conductivity	$\mu\text{S/cm}$	185 – 210
Total organic carbon (TOC)	mg/L	5.9 – 11
Total nitrogen (TN)	mg/L	4.33 – 8.9
$\text{NH}_4^+\text{-N}$	mg/L	1.9 – 2.9
$\text{PO}_4^{3-}\text{-P}$	mg/L	4.4 – 7.1

Prior to the commencement of this study, the MBR-treated effluent was spiked with the selected pharmaceuticals and pesticides at 5  $\mu\text{g/L}$  each. PS was directly added to the feed media at a concentration of 1 mM after every  $2\times\text{HRT}$ . Concentration of PS was selected based on its performance in preliminary batch experiments at different PS concentrations, *i.e.*, 0–2 mM (Supplementary data Table S2), as well as a comprehensive literature survey [30, 38]. Temperature of MD feed tank and distillate tank was maintained at  $40 \pm 1.5^\circ\text{C}$  and  $20 \pm 0.5^\circ\text{C}$ , respectively. A DCMD system operated without PS dosing served as the ‘control’. The spiked secondary treated wastewater was treated by DCMD with and without PS dosing in continuous-flow mode for a period of 10 d (*i.e.*,  $13\times\text{HRT}$ ).

Duplicate samples from MD feed tank and distillate tank were collected after every  $2\times\text{HRT}$  for micropollutant quantification. In addition, samples were collected on daily basis to measure TOC and TN removal by the control and PS-assisted DCMD. At the start of each experiment with and without PS dosing, 1.5 L of Milli-Q was added in the distillate tank that served as the initial distillate. Thus, TOC, TN and micropollutant concentrations in MD permeate were corrected for dilution by considering the initial working volume of the distillate tank. At the end of DCMD operation with and without PS, MD membranes were collected and characterized by SEM-EDS to gain an in-depth understanding of the fouling control achieved by PS.

## 2.4. Analytical methods

### 2.4.1. Analysis of basic quality parameters

Samples from micropollutant-spiked secondary treated effluent in MD feed tank and distillate tank were collected on daily basis for analysis. TOC and TN concentrations were measured using a TOC/TN- $V_{\text{CSH}}$  analyser (Shimadzu, Japan). TOC and TN removal efficiency by the stand-alone and PS-assisted

DCMD were calculated based on the method described in Section 2.4.2. The pH and conductivity were measured using an Orion 4 Star Plus portable pH/conductivity meter (Thermo Scientific, Waltham, MA, USA)

#### 2.4.2. Analysis of pharmaceuticals and pesticides

Micropollutants were analysed using a Shimadzu LC-MS system (LC-MS 2020) after solid phase extraction (SPE). A detailed description of this method is available elsewhere [39]. Briefly, micropollutants were extracted using 6 mL Oasis HLB cartridges (Waters, Milford, MA, USA). The HLB cartridges were first pre-conditioned with 5 mL dichloromethane and methanol solution (1:1 v/v), 5 mL methanol and 5 mL Milli-Q water. The pH of the samples was adjusted to 2-3 using 2 M H<sub>2</sub>SO<sub>4</sub>, and then loaded onto the cartridges at a flow rate of 1–4 mL/min. The cartridges were dried for 30 min under gentle stream of nitrogen. The extracted samples were eluted using 7 mL methanol and 7 mL dichloromethane and were dried in a water bath at 40°C for 3-4 h. The residues were redissolved in 400 µL methanol for quantification by LC-MS.

The LC-MS system was equipped with an electrospray ionization (ESI) interface, and a Phenomenex Kinetex C8 chromatography column (50 × 4.6 mm) was used for the separation of micropollutants. Milli-Q water buffered with 0.1% (v/v) formic acid, and HPLC grade acetonitrile was used as the mobile phase during the analysis. Mobile phase flow rate and sample injection volume were 0.5 mL/min and 10 µL, respectively. Quantification of acetaminophen, primidone, trimethoprim, sulfamethoxazole, carbamazepine, bezafibrate, atrazine, linuron, and amitriptyline was performed under ESI positive ionization [M+H]<sup>+</sup> mode, while ESI negative ionization [M-H]<sup>-</sup> mode was adopted for pentachlorophenol, diclofenac and triclosan [39]. During the analysis, detector voltage, desolvation line temperature and heating block temperature were kept constant at 0.9 kV, 250°C, and 200°C, respectively. The analysis was conducted in gradient elution mode as shown in Supplementary Data Table S3. High purity nitrogen that acted as both the nebulizing and drying gas was supplied continuously at a flow rate of 1.5 and 10 L/min, respectively. The calibration curves were prepared by analysing the known concentrations of analytes that ranged between 0.1 and 20 µg/L. The correlation coefficient of all the calibration curves was above 0.99.

Removal of micropollutants by PS ( $R_1$ ) and DCMD ( $R_2$ ) was calculated by using Equation (6) and (7), respectively:

$$R_1 = 100 \times \left(1 - \frac{C_{su}}{C_f}\right) \quad \text{Eq. (6)}$$

$$R_2 = 100 \times \left(1 - \frac{C_p}{C_f}\right) \quad \text{Eq. (7)}$$

where,  $C_f$ ,  $C_{su}$  and  $C_p$  are the concentration (ng/L) of a specific pollutant in secondary treated effluent (*i.e.*, storage tank in Figure 1), MD feed and MD permeate, respectively.

The mass of a micropollutant degraded by PS was calculated as follows:

$$C_f \times V_f = (C_{su} \times V_{su}) + (C_p \times V_p) + \text{Mass degraded by PS} \quad \text{Eq. (8)}$$

Where,  $V_f$ ,  $V_{su}$  and  $V_p$  represents the volume of secondary treated effluent, MD feed and permeate, respectively.

#### 2.4.3. Membrane characterization and toxicity of MD permeate

At the end of DCMD operation with and without PS dosing, MD membranes were collected and air-dried in a desiccator. MD membranes were then coated with an ultra-thin gold layer with a sputter coater (SPI Module, West Chester, PA, USA), and were characterised with a scanning electron microscopy (SEM) coupled with energy dispersion spectrometry (EDS) (JCM-600, JEOL, Tokyo, Japan).

Duplicate samples were collected from secondary treated effluent, MD feed and permeate for toxicity analysis at the end of each experiment. Toxicity, expressed as a relative toxicity unit (rTU, the reciprocal of the  $EC_{20}$  value), was analysed by measuring the inhibition of luminescence in the naturally bioluminescent bacteria, *Photobacterium leiognathi*, using the BLT-Screen as described elsewhere [40].

#### 2.4.4. PS concentration

The change in PS concentration following its addition to the reaction media was monitored during the operation of PS-assisted DCMD by using a previously developed spectrophotometric method [41]. Briefly, two solutions were prepared before measuring PS concentration. Solution-1 was the PS stock solution (100 mM). Solution-2 was prepared by dissolving 0.2 g  $NaHCO_3$  and 4 g KI in 40 mL Milli-Q water, mixed well and allowed to equilibrate for 15 min. Portions of Solution-1 (*i.e.*, 0.1, 0.2, 0.4, 2 and 4 mL) were separately added to Solution-2 to achieve final PS concentration of 0.25, 0.5, 1, 5 and 10 mM. The standard solutions were incubated on a rotary shaker at 80 rpm for 2 h. Absorbance of the standard solutions was measured at a wavelength of 352 nm in 1 cm quartz cuvettes using a UV-visible spectrophotometer (DR6000, Hach, Loveland, CO, USA). The coefficient of determination ( $R^2$ ) obtained by drawing the calibration curve was  $>0.98$  (Supplementary data Figure S1). For determining the concentration of PS during the operation of PS-assisted DCMD, 20 mL sample collected from MD feed was added to 40 mL Solution-2, and the resulting solution was incubated for 2 h before measuring its absorbance at 352 nm using a UV-visible spectrophotometer as described above. The concentration of the PS was corrected by multiplying it with the dilution factor of 3.

### 3. Results and discussion

#### 3.1. Mass transfer coefficient ( $K_m$ ) of DCMD

The mass transfer coefficient ( $K_m$ ) of the DCMD system in the current study was determined experimentally using ultrapure Milli-Q water as feed following Equations 3–5. Mass transfer (denoted by  $K_m$  value) during DCMD operation can be affected by concentration and temperature polarization.

Since concentration of salts in Milli-Q water is negligible, the effect of concentration polarization on  $K_m$  could be ignored. Temperature polarization effect has been incorporated in Equations 3–5 for the determination of  $K_m$ . The significance of temperature polarization effect can be assessed by comparing  $K_m$  values at different feed temperatures [9, 10]. Despite the increase in permeate flux (Figure 2a),  $K_m$  reduced with the increase of MD feed temperature from 40 to 50°C (Figure 2). This indicates that temperature polarization effects become severe at high feed temperature, which is consistent with the available literature [10, 42, 43]. Therefore, we operated the DCMD system at a feed temperature of 40°C, resulting in a  $K_m$  value 2.7 L/m<sup>2</sup>.h.Pa.

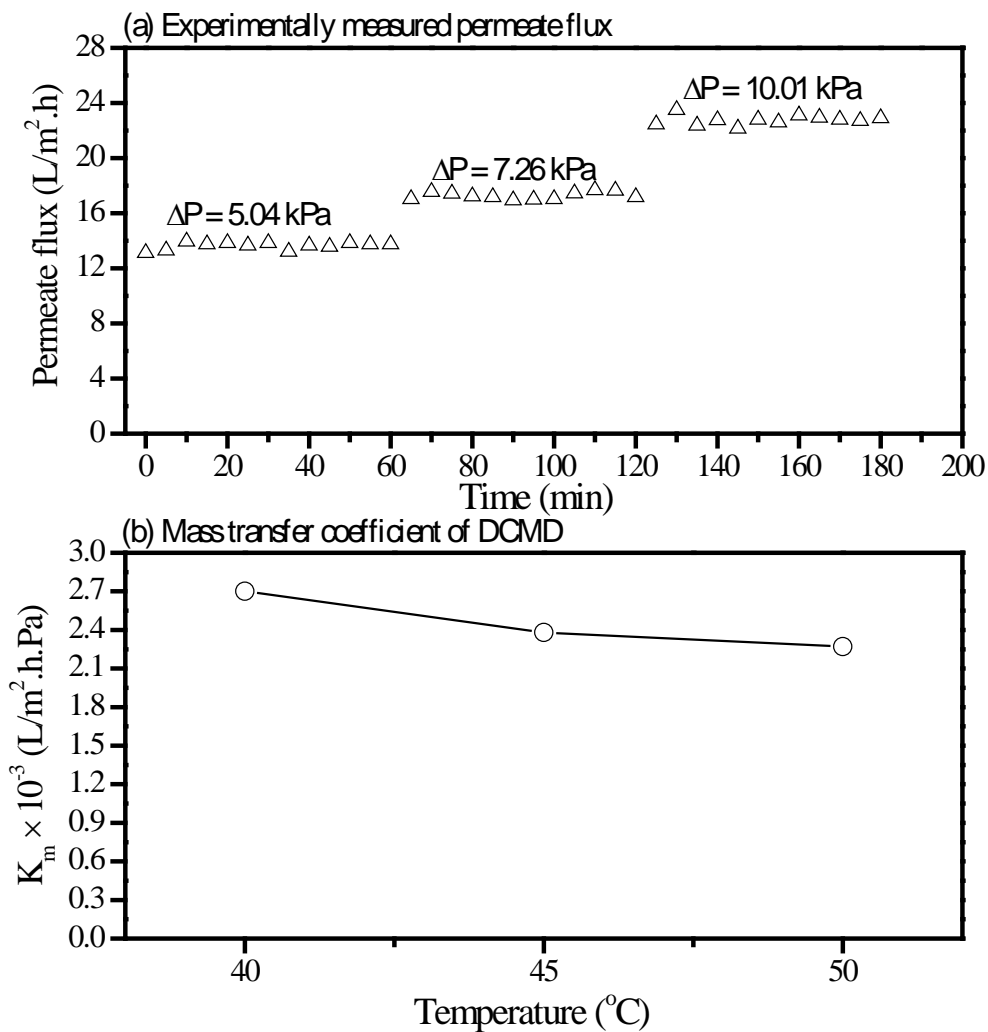


**Figure 2.** Permeate flux (a) and mass transfer coefficient (b) of the DCMD system determined experimentally with Milli-Q water as feed at a temperature of 40, 45 and 50 °C. Temperature of the distillate reservoir was kept at 20 °C, while the cross-flow velocity was maintained at 1 L/min.

### 3.2. Removal of micropollutants

#### 3.2.1. Overall removal by MD and PS-assisted MD

Overall removal of the selected micropollutants by both the standalone and PS-assisted DCMD are presented in Figure 3. In a stand-alone DCMD process, membrane retention is the only mechanism of

micropollutants removal. Because water moves across an MD membrane in vapour form, the extent of micropollutant removal by the membrane is influenced by the water partition coefficient ( $\log D$ ) and vapour pressure of the target pollutant [6]. Noting that  $pK_H = -\log_{10} H$  (where,  $H$  is the Henry's Law constant and is equal to vapour pressure  $\times$  MW/water solubility), in general, micropollutants with a low ' $pK_H / \log D$ ' ratio (*e.g.*, less than 2.5) are partially removed by the MD membrane in a stand-alone DCMD system [7, 44]. In the current study, the stand-alone DCMD achieved micropollutant-specific removal that ranged between 86 and 100%. Out of the 12 selected micropollutants, six including five PPCPs (carbamazepine, trimethoprim, bezafibrate, primidone and acetaminophen) and a pesticide (pentachlorophenol) exhibited removal greater than 98% (Figure 3). For the remaining micropollutants, MD achieved a removal of 86% for atrazine, 91% for triclosan, 92% for amitriptyline, 94% for diclofenac, 95% for sulfamethoxazole, and 96% for linuron (Figure 3). Song et al. [16] investigated the performance of a stand-alone DCMD system for the treatment of anaerobic-MBR permeate containing a mixture of micropollutants. Consistent with the results of the current study, they also reported good but incomplete removal (80-95%) of a few micropollutants such as atrazine, diclofenac, sulfamethoxazole, linuron and triclosan [16].

It is interesting to note that, following PS dosing at a concentration of 1 mM, >99% removal efficiencies were observed for all 12 investigated micropollutants (Figure 3). In previous studies, beneficial effects of integrating an activated sludge-based or enzymatic bioreactor with DCMD have been reported [45]. For instance, the overall micropollutant removal was significantly improved when an enzymatic bioreactor was integrated with a DCMD system [36, 44]. This was attributed to the enzymatic biodegradation of micropollutants and their simultaneous MD retention. The current study demonstrates the benefit of integrating PS-assisted degradation with DCMD for the first time. Further discussion regarding micropollutant degradation is provided in Section 3.2.2.



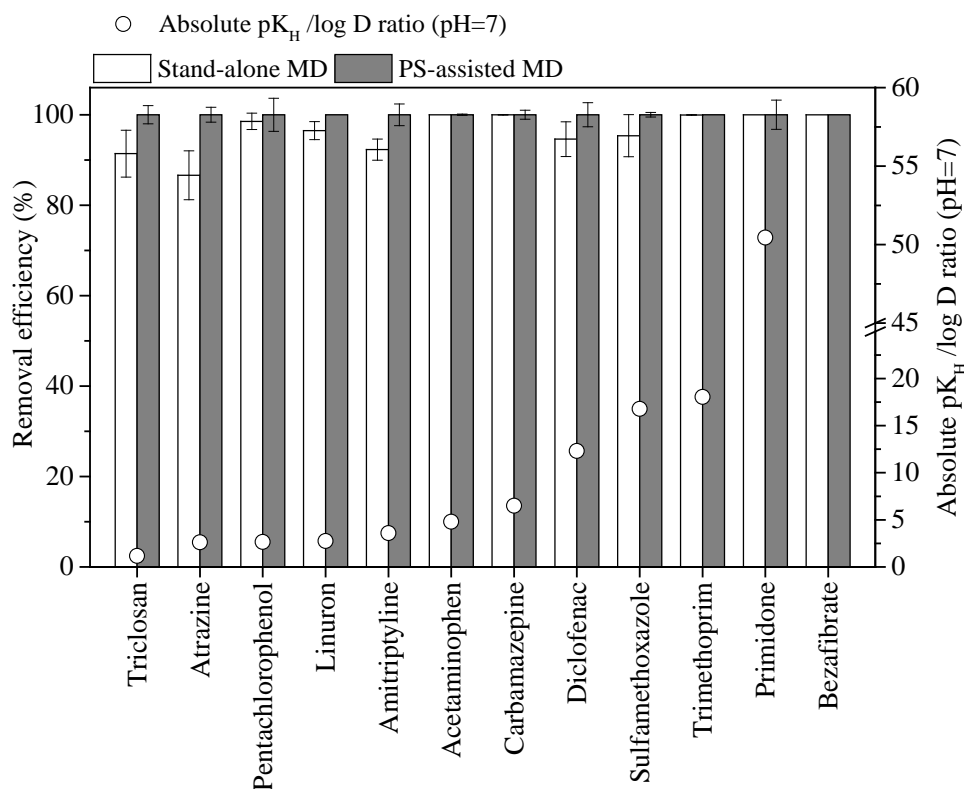


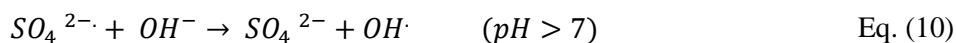
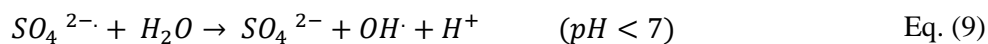
**Figure 3.** Performance of the stand-alone DCMD and PS-assisted DCMD for the overall removal of the selected micropollutants arranged based on  $pK_H / \log D$ . Membrane retention was the only mechanism of micropollutant removal in the stand-alone DCMD, while both degradation and membrane retention contributed to micropollutant removal by PS-assisted DCMD. Operating conditions: the initial micropollutant concentration was  $5 \mu\text{g/L}$ ; PS dose was  $1 \text{ mM}$ ; temperature of the MD feed (with and without PS) and the distillate (permeate) tank was kept at  $40$  and  $20 \text{ }^\circ\text{C}$ ; and cross-flow rate was  $1 \text{ L/min}$  (corresponding to cross-flow velocity of  $9 \text{ cm/s}$ ). Mean removal efficiency and standard deviation from five duplicate samples ( $n=10$ ) are presented.

### 3.2.2. Degradation of micropollutants by PS

In a stand-alone DCMD, micropollutants accumulate within the feed following their retention by the MD membrane. Over time, this can affect micropollutant retention. This also requires additional intensive treatment of MD-concentrate that needs to be periodically purged from the system. Thus, intermittent PS dosing was investigated for micropollutant degradation to reduce their accumulation in feed during DCMD operation.

Following the absorption of heat, breaking of the peroxide bond (O–O) that bridges the sulphur atoms in persulfate occurs, resulting in the formation of two  $\text{SO}_4^{\cdot -}$  radicals as shown in Equation 1 [30]. Depending on wastewater characteristics, persulfate or  $\text{SO}_4^{\cdot -}$  radicals may react with water and/or organics to form secondary radicals that can also contribute to degradation of organic impurities [30, 46].  $\text{SO}_4^{\cdot -}$  radicals can react with water to form hydroxyl ( $\text{OH}^{\cdot}$ ) radicals, but the abundance of the  $\text{SO}_4^{\cdot -}$  and  $\text{OH}^{\cdot}$  radicals is governed by the pH of reaction media (Equation 9 and 10). Under acidic conditions ( $\text{pH}<7$ ),  $\text{SO}_4^{\cdot -}$  radicals are the dominant species, while  $\text{OH}^{\cdot}$  is the primary reactive species under basic

conditions (pH>7). At neutral pH, both  $SO_4^{\cdot-}$  and  $OH^{\cdot}$  radicals contribute equally to pollutant degradation [47]. Since the pH of the secondary treated effluent in this study ranged between 6.84 and 7.2, both  $SO_4^{\cdot-}$  and  $OH^{\cdot}$  radicals were responsible for the degradation of micropollutants in this study.



A mass balance (Equation 8) reveals that heat-activated PS achieved 25-100% degradation of the micropollutants (Figure 4). The tested micropollutants can be divided into three categories based on the performance of the heat-activated PS: (i) 90-100% degradation of four PPCPs, namely amitriptyline, trimethoprim, bezafibrate and acetaminophen; (ii) 60-90% degradation of three pesticides (atrazine, linuron and pentachlorophenol) and four PPCPs (carbamazepine, triclosan, sulfamethoxazole and primidone); and (iii) less than 25% degradation of the pharmaceutical compound diclofenac (Figure 4). Similar to biodegradation [5, 48-50], degradation of micropollutants by the heat-activated PS appears to be governed by their chemical structure (*e.g.*, presence of EWGs and/or EDGs). For instance, micropollutants such as amitriptyline, trimethoprim and bezafibrate that contain amine ( $-NH_2$ ), alkyl ( $-R$ ) or acyl ( $-COR$ ) EDGs were readily degraded (Figure 4). This is because sulphate radicals are electrophilic and can achieve faster degradation of pollutants containing strong EDGs [51]. However, even some of the compounds with strong EWGs underwent significant degradation. Of particular interest was the significantly higher PS-mediated degradation of pesticides, particularly atrazine and linuron, compared to biodegradation by conventional activated sludge and fungal enzymes [5, 48, 49].

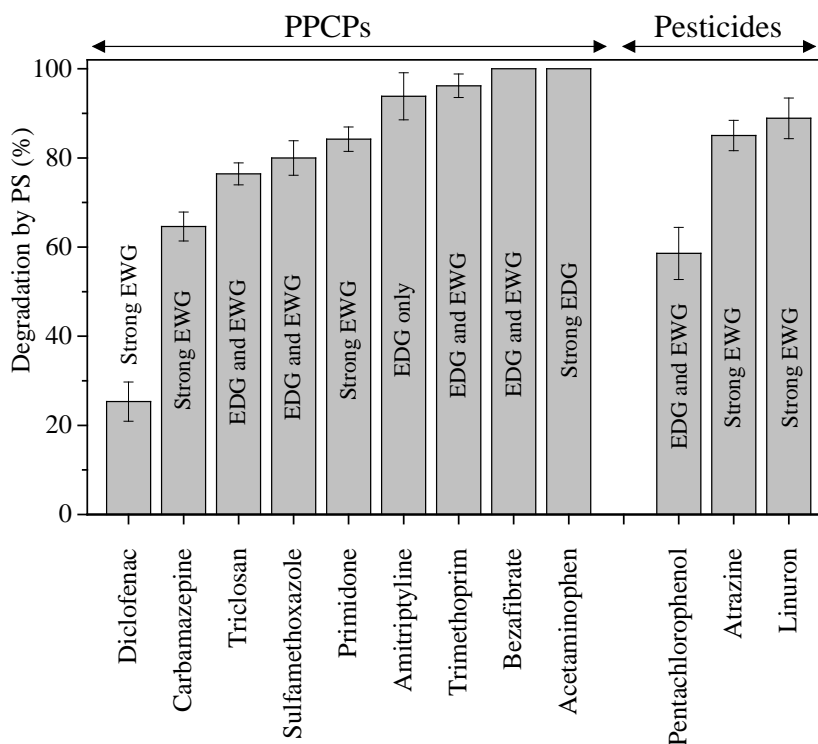


**Figure 4.** Degradation of the selected micropollutants during the treatment of secondary treated effluent by PS-assisted DCMD. Each bar is labelled based on the presence of EDGs and/or EWGs in the molecule of micropollutants. The results are presented as average  $\pm$  standard deviation (n=10). Operating conditions are presented in the caption of Figure 3.

Literature on the degradation of micropollutants by heat-activated PS is scarce, and to date has been generally focused on PS activation routes in the presence of a single micropollutant. For instance, Deng et al. [34] reported only 12% degradation of carbamazepine following 2 h treatment with heat-activated PS at a PS concentration and operating temperature of 1 mM and 40°C, respectively. In a study by Ji et al. [35], PS (1 mM) activated by heat at 40°C achieved 20% atrazine degradation after an incubation time of 120 h. Ji et al. [52] observed complete degradation of the antibiotic sulfamethoxazole within 8 h at 50°C. These previous experiments were done in batch mode. Instead of a single micropollutant, performance of heat-activated PS for the degradation of a dozen of micropollutants in their mixture was assessed for the first time in this study. Furthermore, this is the first set of data from a reactor operated in continuous-feeding mode. Although a direct comparison with previous data [34, 35] is not recommended due to the differences in experimental setup, higher degradation efficiencies observed in the current study are worth noting.

Compared to an integrated activated sludge-DCMD system, degradation of a few micropollutants in the PS-assisted DCMD was more efficient. For instance, Wijekoon et al. [36] reported less than 30% removal for diclofenac, atrazine and carbamazepine in an activated sludge-DCMD system. Although diclofenac removal by both systems was comparable, PS-assisted DCMD in this study achieved 64% degradation of carbamazepine, and 85% degradation of atrazine (Figure 4). Future studies are recommended to systematically compare biodegradation vs. advanced oxidation-assisted DCMD process. However, that is beyond the scope of this study.

### *3.2.3. Fate of micropollutants*

The overall micropollutant removal by the PS-assisted DCMD was governed by degradation and membrane retention. Heat-activated PS achieved over 60% degradation of all but one tested micropollutant (diclofenac) (Figure 4). In fact, around two-third of the compounds were degraded with an efficiency greater than 80% by heat-activated PS alone. Thus, degradation by PS was the main mechanism of removal for all micropollutants, except for diclofenac. Nevertheless, membrane retention also contributed significantly (3-74%) for producing a micropollutant-free (<0.1  $\mu\text{g/L}$ ) permeate stream (Figure 5). On the other hand, membrane retention was solely responsible for the removal of micropollutants in the stand-alone DCMD. When compared, the fate of the micropollutants in the investigated systems (Figure 5) shows the clear advantage of the PS-assisted DCMD for effective micropollutant removal and for producing a less-concentrated waste stream due to PS-assisted degradation. Previous studies have reported the fate of micropollutants in biodegradation-coupled

membrane systems [36, 44]. However, this is the first study to elucidate the fate and distribution of micropollutants during PS-assisted DCMD treatment.

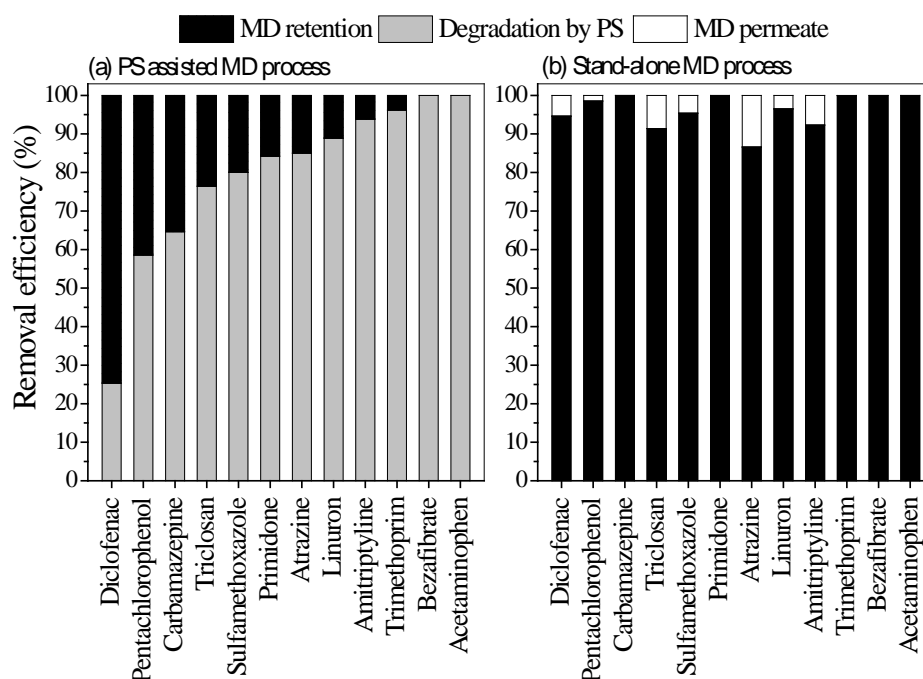


**Figure 5.** Fate of the micropollutants in (a) PS-assisted DCMD; and (b) stand-alone DCMD operated separately for a period of  $13 \times \text{HRT}$ . The MD feed tank was covered to avoid evaporation loss during all experiments. Operating conditions are presented in the caption of Figure 3.

### 3.2.4. Depletion of PS during DCMD operation

The concentration of the PS added to the DCMD reactor was monitored to determine if recurrent dosing of PS was required. Only a few studies have investigated the depletion of sulphate radicals during micropollutant oxidation [46, 53-55]. The radicals (*e.g.*,  $\text{SO}_4^{\cdot -}$  and  $\text{OH}^{\cdot}$ ) formed following PS activation by heat not only can react with the target pollutants but can also react with other radicals and non-target pollutants. The scavenging reactions (*i.e.*, radical-radical and radical-nontarget) produce secondary radicals that can take part in the degradation process. However, scavenging reactions deplete PS by converting the  $\text{SO}_4^{\cdot -}$  radicals into sulphate ions [46, 51]. Depletion of PS necessitates its intermittent dosing to maintain the performance of the oxidation process. In this study, the concentration of persulfate was observed to be reduced by almost 50% over a period of  $2 \times \text{HRT}$  (*see* Supplementary Data Figure S2). Thus, intermittent dosing of PS after every  $2 \times \text{HRT}$  was applied to reinstate PS concentration to 1 mM and maintain PS-mediated degradation. Although the addition of PS would increase the operating cost of the treatment system, it is compensated generously by: (i) achieving improved micropollutant removal in DCMD; (ii) reducing the accumulation of organic impurities in the feed of DCMD (See section 3.3); and (iii) significantly mitigating membrane fouling (See section 3.4).

### 3.3. Removal of TOC and TN

Overall removal of bulk organics was monitored via TOC and TN concentration in the MD feed and permeate (distillate). TOC and TN removal by the stand-alone and PS-assisted DCMD was consistently above 99% as shown in Figure 6, thus ensuring high quality treated effluent. However, effective retention of TOC and TN during continuous feeding also means their accumulation in MD feed tank (*i.e.*, MD reactor), which may cause severe membrane fouling [16]. This aspect is more comprehensively discussed in Section 3.4.

Persulfate and  $\text{SO}_4^{\cdot-}$  radicals can directly react with organic impurities (*e.g.*, humic substances) to either degrade them or form organic radicals. The complex combination of  $\text{SO}_4^{\cdot-}$  chain propagation and termination reactions govern the overall degradation of organic impurities [30, 56, 57]. On the other hand, depending on the pH of the wastewater, persulfate can oxidize all forms of nitrogen to nitrate-nitrogen ( $\text{NO}_3^-$ -N). Accordingly, persulfate oxidation method has been reported as an effective alternate method for the determination of total nitrogen in a wide range of matrices including water and soil [58, 59]. In a previous study, dissolved organic carbon removal by UV-activated PS (0.6 mM) was reported to be 80% after an irradiation time of 3 h [21]. Depending on the dose of PS, Deng and Ezyske [60] achieved chemical oxygen demand and ammonia-nitrogen removal of up to 95 and 80%, respectively, from landfill leachate. Consistent with previous studies, the current study shows significant TOC and TN removal by heat-activated PS.

In this study, following effective retention by MD membrane, up to 40 and 70% degradation of TN and TOC, respectively, was achieved by the PS-assisted DCMD, which significantly reduced the accumulation of these impurities in the MD reactor (Figure 6). At the end of operation, TOC and TN concentrations in the MD reactor of the stand-alone DCMD (without PS) were 84 and 62 mg/L, respectively. By contrast, concentrations of TOC and TN were 22 and 33 mg/L, respectively at the conclusion of the experiment with the PS-assisted DCMD system (Figure 6). This is the first study demonstrating the advantage of combining PS oxidation with the MD process. Particularly, operating the DCMD system in a continuous flow (*i.e.*, continuous feeding) mode helped demonstrate the effectiveness of PS in significantly reducing the accumulation of organics within the reactor.

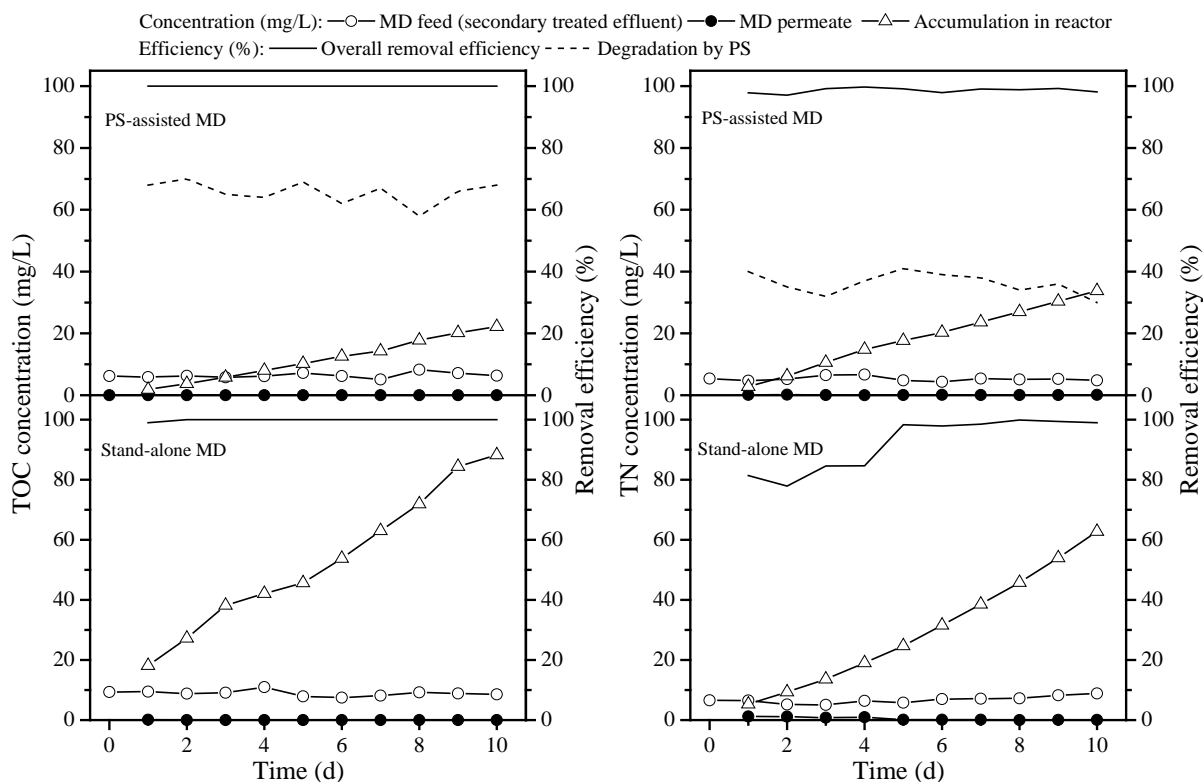


**Figure 6.** TOC and TN removal by the PS-assisted MD and stand-alone MD systems operated separately for a period of  $13 \times \text{HRT}$ . Operating conditions are presented in the caption of Figure 3.

### 3.4. Permeate flux and membrane fouling characterization

Permeate flux of both stand-alone and PS-assisted DCMD was monitored continuously throughout their operation in continuous-flow mode (Figure 7). Permeate flux of the stand-alone DCMD reduced gradually at a rate of  $0.5 \text{ L/m}^2 \cdot \text{h/d}$ , dropping to 72% of the initial flux within 10 days (*i.e.*,  $13 \times \text{HRT}$ ) of operation. Conversely, the flux of the PS-assisted DCMD reduced at a much slower rate of  $0.19 \text{ L/m}^2 \cdot \text{h/d}$  for the first four days, beyond which the flux almost stabilised for the remainder of the PS-DCMD operation (Figure 7).

Significant flux reduction during the stand-alone DCMD operation can be attributed to membrane fouling. A fouling layer formed on the membrane surface can significantly affect permeate flux by reducing the active area of membrane surface for effective mass transfer [16, 61]. The much slower flux reduction for PS-DCMD can be attributed to the degradation of TOC (approximately 70%, Figure 6) achieved by heat-activated PS, which reduced TOC accumulation in the feed of the PS-assisted DCMD system.

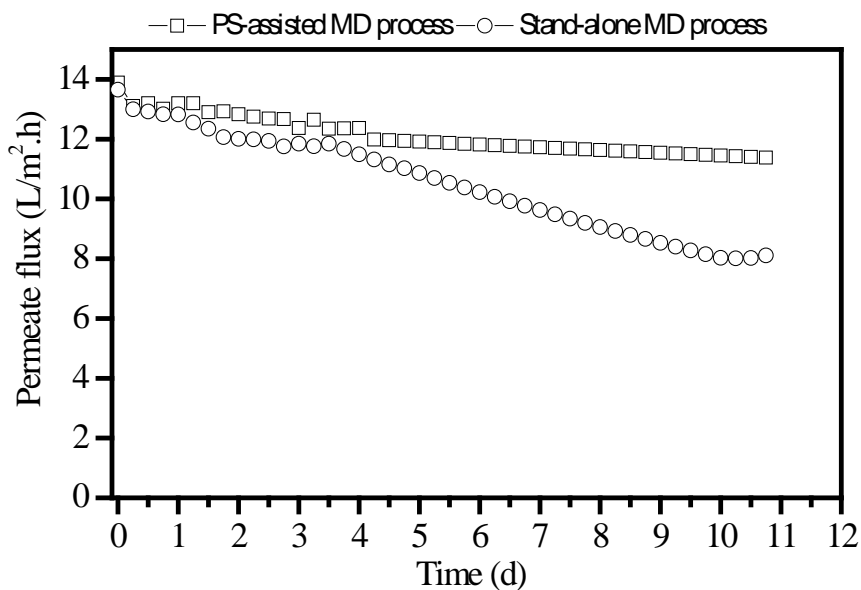


**Figure 7.** Variations in the permeate flux as a function of time. Operating conditions are given in the caption of Figure 3.

To derive deeper insights into the fouling phenomenon, the fouling layer formed on the membrane surface was characterised by SEM-EDS. As shown in Figure 8, during the standalone DCMD operation, a dense fouling layer formed on the membrane that almost uniformly covered the surface. On the other hand, during the PS-assisted DCMD operation, the fouling layer on the membrane was distributed unevenly and covered a significantly smaller surface area. The EDS spectra revealed that the fouling layers were mainly composed of carbon, oxygen and iron. However, the comparison of EDS spectra suggests that the abundance of carbon and oxygen (main constituents of organic impurities) was significantly higher (almost double) in the fouling layer of the membrane collected from the standalone DCMD system. A similar composition of fouling layer was reported when standalone DCMD was operated for the treatment of anaerobic-MBR permeate [16]. Song et al. [16] additionally observed the deposition of phosphorous on the MD membrane. However, in the current study, phosphorous was not detected in the membrane fouling layer. This can be due to the low concentration (*i.e.*, 4.4-7.1 mg PO<sub>4</sub><sup>3-</sup>-P/L) of phosphorous in the secondary treated effluent used in the current study compared to that reported for anaerobically treated effluent in the study by Song et al. [16], *i.e.*, approximately 200 mg PO<sub>4</sub><sup>3-</sup>-P/L.

MD membrane flux reduction can be also caused by accumulation of salts leading to concentration polarization [9]. However, in this study, at the end of the operation, the conductivity of the feed increased from 200 to 2050 μS/cm in case of the standalone DCMD system, which is comparable to the increase observed for the PS-assisted DCMD system (*i.e.*, from 190 to 2940 μS/cm). Noting that both membranes were exposed to similar salt levels, but the flux decline was more severe in case of the standalone DCMD membrane, it is evident that under the operating conditions of this study, salt accumulation did not affect the permeate flux of both systems. Furthermore, membrane pore wetting

phenomenon did not occur for any of the membranes, which is evident from the effective conductivity removal (above 99%) by MD membrane in all experiments.

It is noteworthy that the fouling layer on the membrane could potentially influence the degree of removal of dissolved constituents including micropollutants. For example, for nanofiltration, membrane fouling may cause different changes in hydrophobicity, surface charge, and effective pore size of the membrane, which may lead to reduced rejection depending on the membrane evaluated and the charge of the compound [62]. Also, in the presence of a fouling layer, polymeric forward osmosis membranes may swell due to elevated electroneutrality, reducing rejection of hydrophilic non-ionic micropollutants [63]. However, our study shows that despite significant fouling, the micropollutant removal by the MD membrane was fairly stable throughout the operation period (Figure 3).

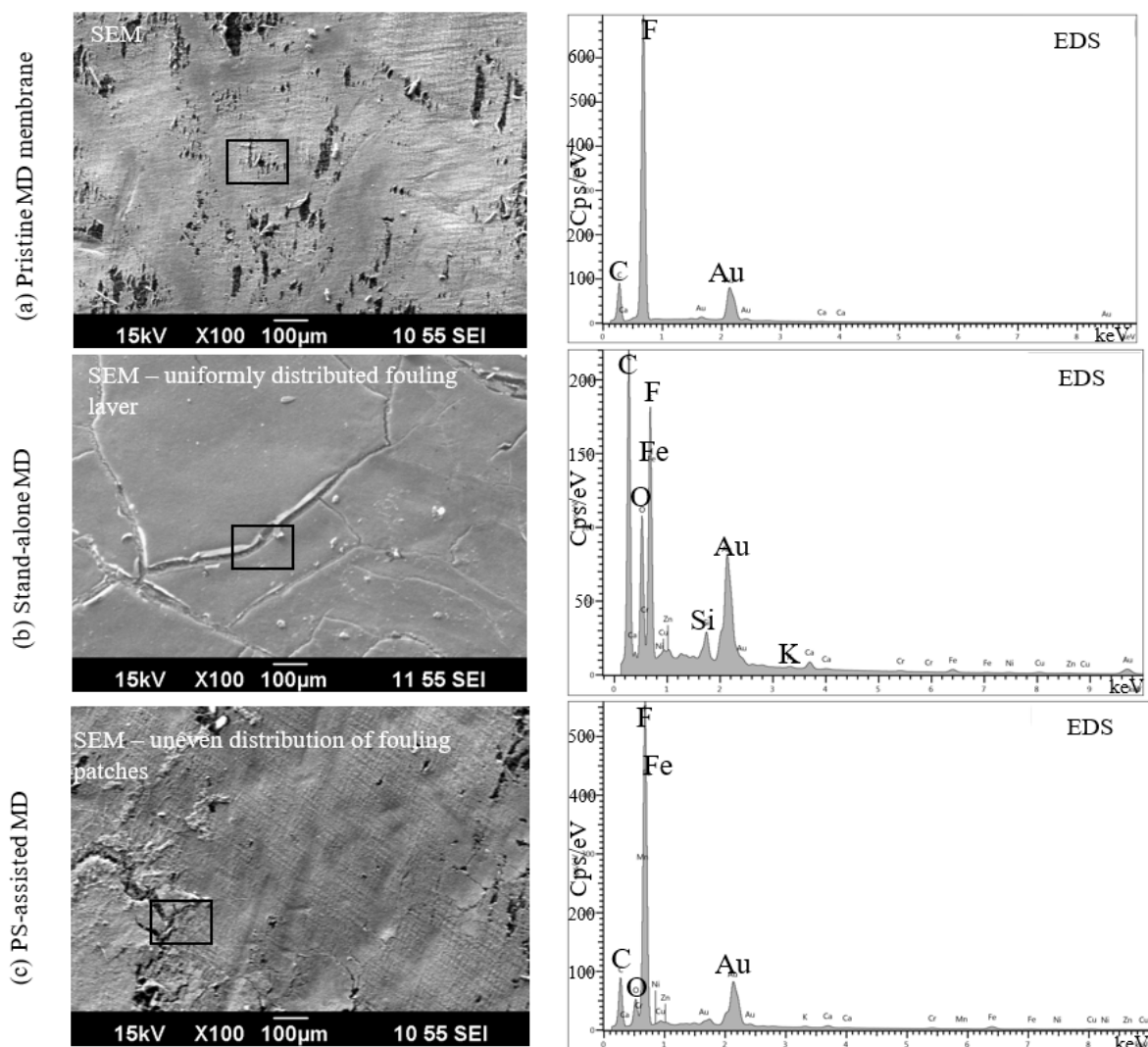


**Figure 8.** SEM images and EDS spectra of pristine MD membrane (a) and fouled membrane collected at the end of experiment with the stand-alone MD (b) and PS-assisted MD (c) systems. Operating conditions of DCMD systems are given in the caption of Figure 3.



### 3.5. Toxicity of treated effluent

Mechanisms of micropollutant removal by sulphate radicals include hydrogen abstraction, electron transfer and addition of double bond [30]. It is important to confirm that the products of PS-mediated transformation of micropollutants are not significantly more toxic. Since a mixture of 12 micropollutants was selected for this study, it is not possible to link the transformation products to the parent compounds. Thus, instead of monitoring individual transformation products, the overall toxicity of the feed water and final effluent were monitored in this study. Previously, toxicity of the effluent following treatment with activated-PS has been assessed by monitoring the inhibition of bioluminescence in different bacterial species. For instance, Zhang et al. [38] assessed the toxicity of the reaction media following treatment of a test solution containing carbamazepine with UV-activated PS by measuring the bioluminescence inhibition in a freshwater bacteria, *viz* *Vibrio qinghaiensis sp.* They reported that the toxicity of the reaction media reduced by 35% after 60 min treatment with UV-activated PS. In another study by Qi et al. [64], toxicity of a sulfamethoxazole solution treated by microwave-activated PS was measured by monitoring the bioluminescence inhibition in three bacterial species, namely, *Vibrio fischeri*, *Photobacterium phosphoreum*, and *Vibrio qinghaiensis*. They also reported significant reduction in toxicity (~90%) following PS treatment. Compared to the available studies, the current study provides new insights into treated effluent toxicity given that a secondary treated wastewater containing 12 micropollutants was treated by operating a PS-assisted DCMD in a continuous-flow mode.

The bioluminescent bacteria *Photobacterium leiognathi* was used in this study to monitor effluent toxicity. Our analysis indicates that the reactor media toxicity for both the stand-alone and PS-assisted DCMD slightly increased at the end of their operation (Table 3), and that the toxicity of the PS-assisted DCMD reactor media (6.3-6.5 rTU, n=2) was higher than that of the stand-alone DCMD (3.4-3.9 rTU, n=2). This suggests that PS itself and/or the transformation products originating from PS-mediated degradation of the organics present in the feed (*i.e.*, effluent organic matter and spiked micropollutants) was slightly more toxic than the feed. Whatever those compounds (whether PS, or intermediate micropollutant transformation products) were, they did not pass into the permeate, and the MD permeate (*i.e.*, the final effluent) was not toxic to bacteria (below the assay limit of detection, <1 rTU) (Table 3).

**Table 3.** Toxicity, expressed as relative toxic unit (rTU), of different samples. The limit of detection of the toxicity assay was 1 rTU. Number of samples, n = 2.

Sample description	Toxicity (rTU)
MD feed ( <i>i.e.</i> , Secondary treated effluent + micropollutants)	<1 – 2.4
Reactor media of the stand-alone DCMD <sup>a</sup>	3.4 – 3.9
Reactor media of the PS-assisted DCMD <sup>a</sup>	6.3 – 6.5
DCMD permeate	<1

<sup>a</sup>at the end of continuous operation for a period of 13×HRT

#### 4. Conclusions

In this study, persulfate (PS) oxidation was integrated with the direct contact membrane distillation (DCMD) process for effective degradation of 12 recalcitrant micropollutants from secondary treated effluent. Depending on the molecular structure and hydrophobicity of the micropollutants, PS dosing at a concentration of 1 mM resulted in degradation of 25 to >99% (median = 84%) degradation. This led to the consistent achievement of >99% removal of all the micropollutants from the MD permeate (*i.e.*, final effluent) during continuous operation, without production of toxic transformation products in the DCMD permeate. Evidenced by 70% TOC and 40% TN removals, activated PS degraded other organic impurities, along with micropollutants present in MD feed (*i.e.*, secondary treated effluent). Accordingly, during continuous operation of the PS-assisted DCMD, organics accumulation in the reactor media was significantly reduced. This in turn helped minimize membrane fouling.

#### Acknowledgment:

This research has been conducted with the support of an Australian Commonwealth Government Research Training Program Scholarship. This study was partially funded by the Global Challenges Program, University of Wollongong, Australia.

#### References

- [1] Y. Luo, W. Guo, H.H. Ngo, L.D. Nghiem, F.I. Hai, J. Zhang, S. Liang, X.C. Wang, A review on the occurrence of micropollutants in the aquatic environment and their fate and removal during wastewater treatment, *Sci. Total Environ.*, 473 (2014) 619-641.
- [2] F. Hai, S. Yang, M. Asif, V. Sencadas, S. Shawkat, M. Sanderson-Smith, J. Gorman, Z.-Q. Xu, K. Yamamoto, Carbamazepine as a possible anthropogenic marker in water: occurrences, toxicological effects, regulations and removal by wastewater treatment technologies, *Water*, 10 (2018) 107.
- [3] S.D. Melvin, F.D. Leusch, Removal of trace organic contaminants from domestic wastewater: A meta-analysis comparison of sewage treatment technologies, *Environ. Int.*, 92 (2016) 183-188.
- [4] F.I. Hai, L.D. Nghiem, S.J. Khan, W.E. Price, K. Yamamoto, Wastewater reuse: Removal of emerging trace organic contaminants, in: F.I. Hai, K. Yamamoto, C. Lee (Eds.) *Membrane Biological Reactors: Theory, Modeling, Design, Management and Applications to Wastewater Reuse*, IWA publishing, London, United Kingdom 2014, pp. 165-205. (ISBN: 9781780400655).
- [5] N. Tadkaew, F.I. Hai, J.A. McDonald, S.J. Khan, L.D. Nghiem, Removal of trace organics by MBR treatment: the role of molecular properties, *Water Res.*, 45 (2011) 2439-2451.
- [6] M.B. Asif, A.J. Ansari, S.-S. Chen, L.D. Nghiem, W.E. Price, F.I. Hai, Understanding the mechanisms of trace organic contaminant removal by high retention membrane bioreactors: a critical review, *Environ. Sci. Pollut. Res.*, (2018) 1-16. (DOI: 10.1007/s11356-11018-13256-11358).
- [7] K.C. Wijekoon, F.I. Hai, J. Kang, W.E. Price, T.Y. Cath, L.D. Nghiem, Rejection and fate of trace organic compounds (TrOCs) during membrane distillation, *J. Membr. Sci.*, 453 (2014) 636-642.
- [8] T.L.S. Silva, S. Morales-Torres, C.M.P. Esteves, A.R. Ribeiro, O.C. Nunes, J.L. Figueiredo, A.M.T. Silva, Desalination and removal of organic micropollutants and microorganisms by membrane distillation, *Desalination*, 437 (2018) 121-132.
- [9] A. Alkudhiri, N. Darwish, N. Hilal, Membrane distillation: A comprehensive review, *Desalination*, 287 (2012) 2-18.

- [10] H.C. Duong, F.I. Hai, A. Al-Jubainawi, Z. Ma, T. He, L.D. Nghiem, Liquid desiccant lithium chloride regeneration by membrane distillation for air conditioning, *Sep. Purif. Technol.*, 177 (2017) 121-128.
- [11] C.R. Martinetti, A.E. Childress, T.Y. Cath, High recovery of concentrated RO brines using forward osmosis and membrane distillation, *J. Membr. Sci.*, 331 (2009) 31-39.
- [12] F. Li, J. Huang, Q. Xia, M. Lou, B. Yang, Q. Tian, Y. Liu, Direct contact membrane distillation for the treatment of industrial dyeing wastewater and characteristic pollutants, *Sep. Purif. Technol.*, 195 (2018) 83-91.
- [13] D. Winter, J. Koschikowski, M. Wiegand, Desalination using membrane distillation: Experimental studies on full scale spiral wound modules, *J. Membr. Sci.*, 375 (2011) 104-112.
- [14] L. Camacho, L. Dumée, J. Zhang, J.-d. Li, M. Duke, J. Gomez, S. Gray, Advances in membrane distillation for water desalination and purification applications, *Water*, 5 (2013) 94-196.
- [15] L. Han, T. Xiao, Y.Z. Tan, A.G. Fane, J.W. Chew, Contaminant rejection in the presence of humic acid by membrane distillation for surface water treatment, *J. Membr. Sci.*, 541 (2017) 291-299.
- [16] X. Song, W. Luo, J. McDonald, S.J. Khan, F.I. Hai, W.E. Price, L.D. Nghiem, An anaerobic membrane bioreactor–membrane distillation hybrid system for energy recovery and water reuse: Removal performance of organic carbon, nutrients, and trace organic contaminants, *Sci. Total Environ.*, 628 (2018) 358-365.
- [17] D. Metcalfe, P. Jarvis, C. Rockey, S. Judd, Pre-treatment of surface waters for ceramic microfiltration, *Sep. Purif. Technol.*, 163 (2016) 173-180.
- [18] H. Huang, K. Schwab, J.G. Jacangelo, Pretreatment for low pressure membranes in water treatment: a review, *Environ. Sci. Technol.*, 43 (2009) 3011-3019.
- [19] H. Vatankhah, C.C. Murray, J.W. Brannum, J. Vanneste, C. Bellona, Effect of pre-ozonation on nanofiltration membrane fouling during water reuse applications, *Sep. Purif. Technol.*, 205 (2018) 203-211.
- [20] M. Park, T. Anumol, J. Simon, F. Zraick, S.A. Snyder, Pre-ozonation for high recovery of nanofiltration (NF) membrane system: Membrane fouling reduction and trace organic compound attenuation, *J. Membr. Sci.*, 523 (2017) 255-263.
- [21] J. Tian, C. Wu, H. Yu, S. Gao, G. Li, F. Cui, F. Qu, Applying ultraviolet/persulfate (UV/PS) pre-oxidation for controlling ultrafiltration membrane fouling by natural organic matter (NOM) in surface water, *Water Res.*, 132 (2018) 190-199.
- [22] D. Wei, Y. Tao, Z. Zhang, L. Liu, X. Zhang, Effect of in-situ ozonation on ceramic UF membrane fouling mitigation in algal-rich water treatment, *J. Membr. Sci.*, 498 (2016) 116-124.
- [23] C.-H. Lai, Y.-C. Chou, H.-H. Yeh, Assessing the interaction effects of coagulation pretreatment and membrane material on UF fouling control using HPSEC combined with peak-fitting, *J. Membr. Sci.*, 474 (2015) 207-214.
- [24] K. Kimura, Y. Oki, Efficient control of membrane fouling in MF by removal of biopolymers: Comparison of various pretreatments, *Water Res.*, 115 (2017) 172-179.
- [25] S. Shao, H. Liang, F. Qu, K. Li, H. Chang, H. Yu, G. Li, Combined influence by humic acid (HA) and powdered activated carbon (PAC) particles on ultrafiltration membrane fouling, *J. Membr. Sci.*, 500 (2016) 99-105.
- [26] H. Wang, M. Park, H. Liang, S. Wu, I.J. Lopez, W. Ji, G. Li, S.A. Snyder, Reducing ultrafiltration membrane fouling during potable water reuse using pre-ozonation, *Water Res.*, 125 (2017) 42-51.
- [27] J. Zhang, H. Yu, X. Quan, S. Chen, Y. Zhang, Ceramic membrane separation coupled with catalytic ozonation for tertiary treatment of dyestuff wastewater in a pilot-scale study, *Chem. Eng. J.*, 301 (2016) 19-26.
- [28] M. Bourgin, B. Beck, M. Boehler, E. Borowska, J. Fleiner, E. Salhi, R. Teichler, U. Von Gunten, H. Siegrist, C.S. Mc Ardell, Evaluation of a full-scale wastewater treatment plant upgraded with

ozonation and biological post-treatments: Abatement of micropollutants, formation of transformation products and oxidation by-products, *Water Res.*, 129 (2018) 486-498.

[29] L. Franck-Lacaze, C. Bonnet, S. Besse, F. Lapique, Effects of ozone on the performance of a polymer electrolyte membrane fuel cell, *Fuel Cells*, 9 (2009) 562-569.

[30] L.W. Matzek, K.E. Carter, Activated persulfate for organic chemical degradation: a review, *Chemosphere*, 151 (2016) 178-188.

[31] B.-T. Zhang, Y. Zhang, Y. Teng, M. Fan, Sulfate radical and its application in decontamination technologies, *Crit. Rev. Env. Sci. Tec.*, 45 (2015) 1756-1800.

[32] R.H. Waldemer, P.G. Tratnyek, R.L. Johnson, J.T. Nurmi, Oxidation of chlorinated ethenes by heat-activated persulfate: kinetics and products, *Environ. Sci. Pollut. Res.*, 41 (2007) 1010-1015.

[33] X. Cheng, H. Liang, A. Ding, X. Tang, B. Liu, X. Zhu, Z. Gan, D. Wu, G. Li, Ferrous iron/peroxymonosulfate oxidation as a pretreatment for ceramic ultrafiltration membrane: Control of natural organic matter fouling and degradation of atrazine, *Water Res.*, 113 (2017) 32-41.

[34] J. Deng, Y. Shao, N. Gao, Y. Deng, S. Zhou, X. Hu, Thermally activated persulfate (TAP) oxidation of antiepileptic drug carbamazepine in water, *Chem. Eng. J.*, 228 (2013) 765-771.

[35] Y. Ji, C. Dong, D. Kong, J. Lu, Q. Zhou, Heat-activated persulfate oxidation of atrazine: Implications for remediation of groundwater contaminated by herbicides, *Chem. Eng. J.*, 263 (2015) 45-54.

[36] K.C. Wijekoon, F.I. Hai, J. Kang, W.E. Price, W. Guo, H.H. Ngo, T.Y. Cath, L.D. Nghiem, A novel membrane distillation–thermophilic bioreactor system: Biological stability and trace organic compound removal, *Bioresour. Technol.*, 159 (2014) 334-341.

[37] K.W. Lawson, D.R. Lloyd, Membrane distillation, *J. Membr. Sci.*, 124 (1997) 1-25.

[38] Q. Zhang, J. Chen, C. Dai, Y. Zhang, X. Zhou, Degradation of carbamazepine and toxicity evaluation using the UV/persulfate process in aqueous solution, *J. Chem. Technol. Biotechnol.*, 90 (2015) 701-708.

[39] M. Xie, W.E. Price, L.D. Nghiem, M. Elimelech, Effects of feed and draw solution temperature and transmembrane temperature difference on the rejection of trace organic contaminants by forward osmosis, *J. Membr. Sci.*, 438 (2013) 57-64.

[40] J.P. van de Merwe, F.D. Leusch, A sensitive and high throughput bacterial luminescence assay for assessing aquatic toxicity—the BLT-Screen, *Environ. Sci. Process Impacts*, 17 (2015) 947-955.

[41] C. Liang, C.-F. Huang, N. Mohanty, R.M. Kurakalva, A rapid spectrophotometric determination of persulfate anion in ISCO, *Chemosphere*, 73 (2008) 1540-1543.

[42] L. Martínez-Díez, M.I. Vazquez-Gonzalez, Temperature and concentration polarization in membrane distillation of aqueous salt solutions, *J. Membr. Sci.*, 156 (1999) 265-273.

[43] A. Khalifa, H. Ahmad, M. Antar, T. Laoui, M. Khayet, Experimental and theoretical investigations on water desalination using direct contact membrane distillation, *Desalination*, 404 (2017) 22-34.

[44] M.B. Asif, F.I. Hai, J. Kang, J.P. Van De Merwe, F.D. Leusch, W.E. Price, L.D. Nghiem, Biocatalytic degradation of pharmaceuticals, personal care products, industrial chemicals, steroid hormones and pesticides in a membrane distillation-enzymatic bioreactor, *Bioresour. Technol.*, 247 (2018) 528-536.

[45] M.B. Asif, L.N. Nguyen, F.I. Hai, W.E. Price, L.D. Nghiem, Integration of an enzymatic bioreactor with membrane distillation for enhanced biodegradation of trace organic contaminants, *Int. Biodeterior. Biodegradation*, 124 (2017) 73-81.

[46] R.L. Johnson, P.G. Tratnyek, R.O.B. Johnson, Persulfate persistence under thermal activation conditions, *Environ. Sci. Technol.*, 42 (2008) 9350-9356.

[47] C. Liang, H.-W. Su, Identification of sulfate and hydroxyl radicals in thermally activated persulfate, *Ind. Eng. Chem. Res.*, 48 (2009) 5558-5562.

- [48] M.B. Asif, F.I. Hai, L. Singh, W.E. Price, L.D. Nghiem, Degradation of pharmaceuticals and personal care products by white-rot fungi—A critical review, *Curr. Pollut. Rep.*, 3 (2017) 88-103.
- [49] S. Yang, F.I. Hai, L.D. Nghiem, W.E. Price, F. Roddick, M.T. Moreira, S.F. Magram, Understanding the factors controlling the removal of trace organic contaminants by white-rot fungi and their lignin modifying enzymes: a critical review, *Bioresour. Technol.*, 141 (2013) 97-108.
- [50] M.B. Asif, F.I. Hai, B.R. Dhar, H.H. Ngo, W. Guo, V. Jegatheesan, W.E. Price, L.D. Nghiem, K. Yamamoto, Impact of simultaneous retention of micropollutants and laccase on micropollutant degradation in enzymatic membrane bioreactor, *Bioresour. Technol.*, 267 (2018) 473-480.
- [51] A. Tsitonaki, B. Petri, M. Crimi, H. Mosbæk, R.L. Siegrist, P.L. Bjerg, In situ chemical oxidation of contaminated soil and groundwater using persulfate: a review, *Crit. Rev. Env. Sci. Technol.*, 40 (2010) 55-91.
- [52] Y. Ji, Y. Fan, K. Liu, D. Kong, J. Lu, Thermo activated persulfate oxidation of antibiotic sulfamethoxazole and structurally related compounds, *Water Res.*, 87 (2015) 1-9.
- [53] J.S. Haselow, R.L. Siegrist, M. Crimi, T. Jarosch, Estimating the total oxidant demand for in situ chemical oxidation design, *Remediation*, 13 (2003) 5-16.
- [54] C. Liang, C.J. Bruell, M.C. Marley, K.L. Sperry, Persulfate oxidation for in situ remediation of TCE. II. Activated by chelated ferrous ion, *Chemosphere*, 55 (2004) 1225-1233.
- [55] G.R. Peyton, The free-radical chemistry of persulfate-based total organic carbon analyzers, *Mar. Chem.*, 41 (1993) 91-103.
- [56] C.-W. Wang, C. Liang, Oxidative degradation of TMAH solution with UV persulfate activation, *Chem. Eng. J.*, 254 (2014) 472-478.
- [57] T. Maqbool, S. Bae, J. Hur, Exploring the complex removal behavior of natural organic matter upon N-doped reduced graphene oxide-activated persulfate via excitation-emission matrix combined with parallel factor analysis and size exclusion chromatography, *Chem. Eng. J.*, 347 (2018) 252-262.
- [58] F. Hagedorn, P. Schleppei, Determination of total dissolved nitrogen by persulfate oxidation, *J. Plant Nutr. Soil Sci.*, 163 (2000) 81-82.
- [59] J. Zhou, Z. Chen, S. Li, Oxidation efficiency of different oxidants of persulfate method used to determine total nitrogen and phosphorus in solutions, *Commun. Soil Sci. Plant Anal.*, 34 (2003) 725-734.
- [60] Y. Deng, C.M. Ezyske, Sulfate radical-advanced oxidation process (SR-AOP) for simultaneous removal of refractory organic contaminants and ammonia in landfill leachate, *Water Res.*, 45 (2011) 6189-6194.
- [61] S. Goh, J. Zhang, Y. Liu, A.G. Fane, Fouling and wetting in membrane distillation (MD) and MD-bioreactor (MDBR) for wastewater reclamation, *Desalination*, 323 (2013) 39-47.
- [62] C. Bellona, K. Budgell, D. Ball, K. Spangler, J. Drewes, S. Chellam, Models to predict organic contaminant removal by RO and NF membranes, *IDA Journal*, 3 (2011) 40-44.
- [63] B.D. Coday, B.G. Yaffe, P. Xu, T.Y. Cath, Rejection of trace organic compounds by forward osmosis membranes: a literature review, *Environ. Sci. Technol.*, 48 (2014) 3612-3624.
- [64] C. Qi, X. Liu, C. Lin, X. Zhang, J. Ma, H. Tan, W. Ye, Degradation of sulfamethoxazole by microwave-activated persulfate: Kinetics, mechanism and acute toxicity, *Chem. Eng. J.*, 249 (2014) 6-14.

# Persulfate oxidation-assisted membrane distillation process for micropollutant degradation and membrane fouling control

(Supplementary data)

**Muhammad B. Asif <sup>a</sup>, Zulqarnain Fida <sup>a</sup>, Arbab Tufail <sup>a</sup>, Jason P. van de Merwe <sup>b</sup>, Frederic D.L. Leusch <sup>b</sup>, Biplob K. Pramanik <sup>a,c</sup>, William E. Price <sup>d</sup>, Faisal I. Hai <sup>a,\*</sup>**

<sup>a</sup> Strategic Water Infrastructure Laboratory, School of Civil, Mining and Environmental Engineering, University of Wollongong, Wollongong, NSW 2522, Australia.

<sup>b</sup> Australian Rivers Institute and School of Environment and Science, Griffith University, QLD 4222, Australia.

<sup>c</sup> Civil and Infrastructure Engineering, School of Engineering, RMIT University, Australia

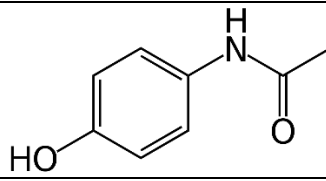
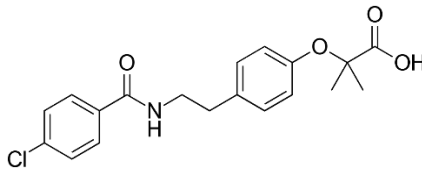
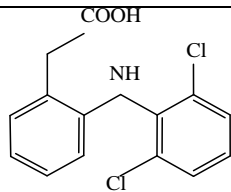
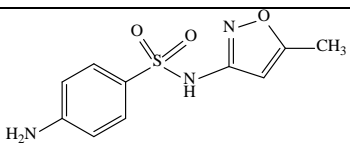
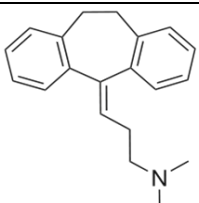
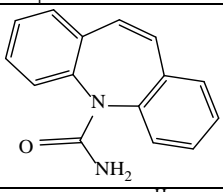
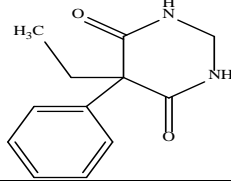
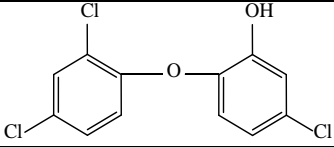
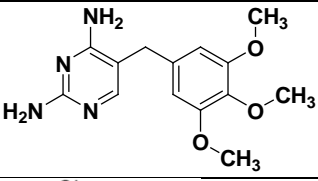
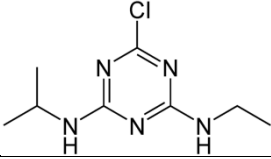
<sup>d</sup> Strategic Water Infrastructure Lab, School of Chemistry, University of Wollongong, Wollongong, NSW 2522, Australia.

\* **Corresponding Author:** [faisal@uow.edu.au](mailto:faisal@uow.edu.au); Tel.: +61-2-42213054

## Table of Contents:

Table S1. Chemical formula and structures of the selected micropollutants .....	2
Table S2: Degradation of the selected micropollutants by PS at different concentrations following an incubation time of 24 h. Results are presented as Average $\pm$ Standard-deviation (n=3).....	4
Table S3: LC-MS analysis eluent gradient time program (adapted from (Xie et al., 2013)).....	5
Figure S1. Calibration curve for the determination of PS concentration.....	6
Figure S2. PS concentration during the treatment secondary effluent by PS-assisted DCMD process	6

**Table S1.** Chemical formula and structures of the selected micropollutants

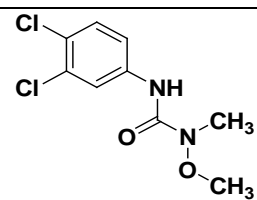
Type	Name	Chemical Formula	MW (g/mol)	Chemical structure
Pharmaceuticals and personal care products (PPCPs)	Acetaminophen	$C_8H_9NO_2$	152	
	Bezafibrate	$C_{19}H_{20}ClNO_4$	362	
	Diclofenac	$C_{14}H_{11}Cl_2NO_2$	296	
	Sulfamethoxazole	$C_{10}H_{11}N_3O_3S$	253	
	Amitriptyline	$C_{20}H_{23}N$	277	
	Carbamazepine	$C_{15}H_{12}N_2O$	236	
	Primidone	$C_{12}H_{14}N_2O_2$	218	
	Triclosan	$C_{12}H_7Cl_3O_2$	290	
Trimethoprim	$C_{14}H_{18}N_4O_3$	290		
Pesticide	Atrazine	$C_8H_{14}ClN_5$	216	

---

Linuron

$C_9H_{10}Cl_2N_2O_2$

249



---

Pentachlorophenol

$C_6HCl_5O$

266

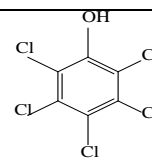




**Table S2:** Degradation of the selected micropollutants by PS at different concentrations following an incubation time of 24 h. Results are presented as Average  $\pm$  Standard-deviation (n=3)

<b>Micropollutants</b>	<b>Degradation (%)</b>			
	PS= 0 mM	PS= 0.5 mM	PS= 1 mM	PS= 2 mM
Sulfamethoxazole	0	45 $\pm$ 3	65 $\pm$ 1	70 $\pm$ 3
Carbamazepine	0	14 $\pm$ 2	69 $\pm$ 2	77 $\pm$ 3
Diclofenac	0	42 $\pm$ 4	69 $\pm$ 4	72 $\pm$ 4

**Table S3:** LC-MS analysis eluent gradient time program. adapted from (Xie et al., 2013)

Time (min)	Eluent B proportion (%) <sup>*</sup>
0	10
6	10
8	23
15	23
16	45
25	45
26	85
30	85
31	10
35	10

<sup>\*</sup> Eluent A contains 0.1% (v/v) formic acid in Milli-Q water; eluent B is acetonitrile.

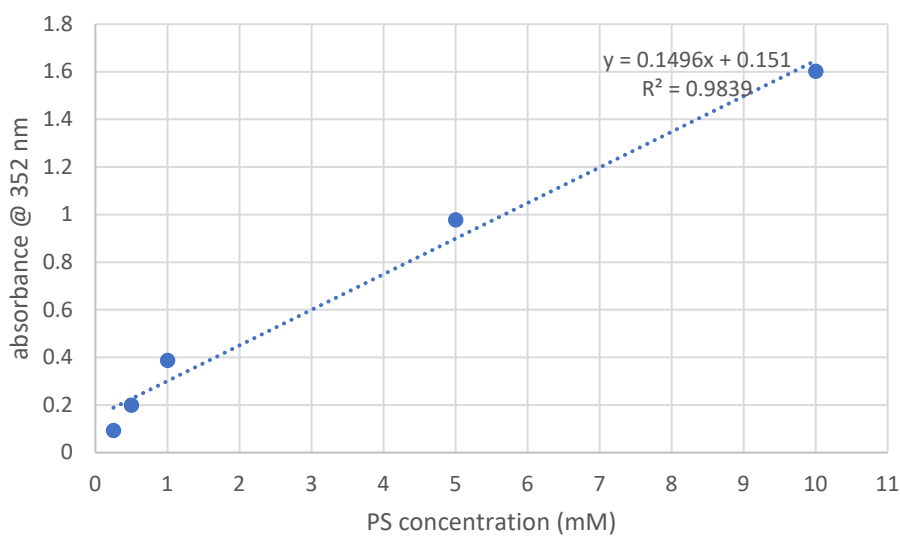


**Figure S1.** Calibration curve for the determination of PS concentration

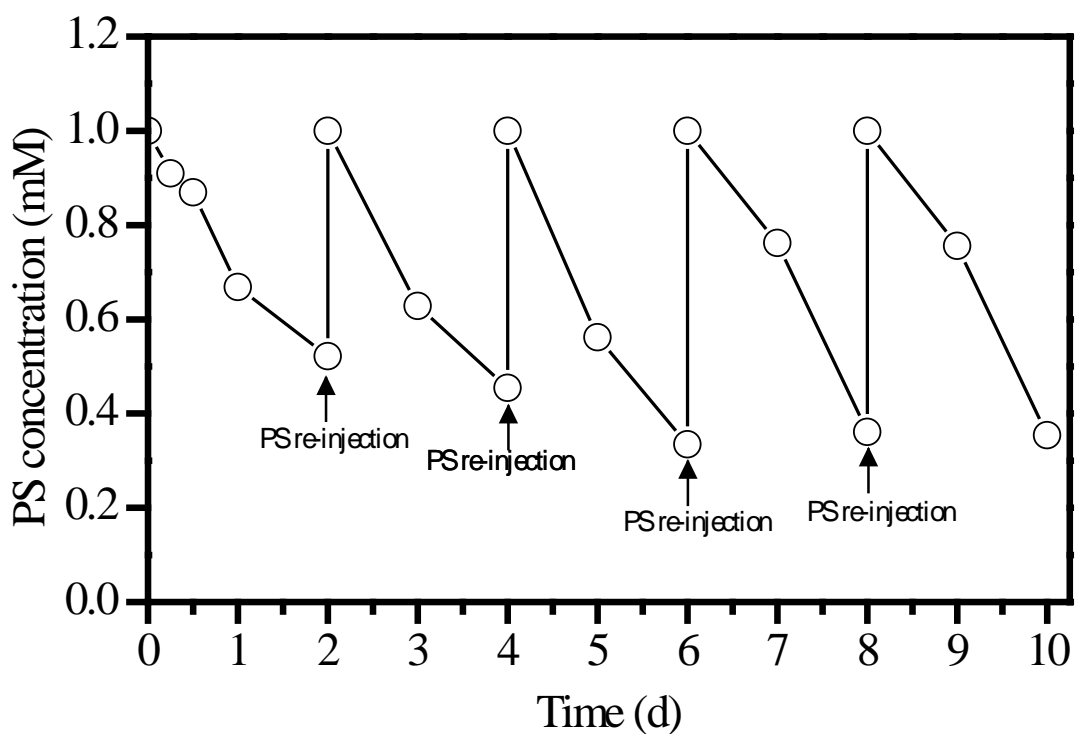


**Figure S2.** PS concentration during the treatment secondary effluent by PS-assisted DCMD process

### References

Xie, M., Price, W.E., Nghiem, L.D., Elimelech, M. 2013. Effects of feed and draw solution temperature and transmembrane temperature difference on the rejection of trace organic contaminants by forward osmosis. *Journal of membrane science*, **438**, 57-64.